

ARTICLE

Study of Electroless Ni-P-CNTs Composite Plating

Ji-lan Kong*, Shang-qi Zhou, Qin Ren, Xi Zhang

College of Materials Science and Engineering, Chongqing University, Chongqing 400030, China

(Dated: Received on December 20, 2005; Accepted on April 7, 2006)

The electroless Ni-P-carbon nanotubes composite plating was studied on the copper substrate. Metallurgical microscope, scanning electronic microscope, X-ray diffractometer and micro hardness tester were used to study the structure, constitution and performance of the electroless Ni-P-carbon nanotubes composite deposit. Experiential results show that, with the increment of carbon nanotubes content in electroless plating solution, the grain size on the sample surface decreases whereas the density of grains and the hardness for composite deposit increases. Moreover, adding carbon nanotubes not only improves the degree of crystallization for the composite deposit but also helps their transformation from the amorphous state to the nanocrystal state.

Key words: Carbon nanotubes, Ni-P, Electroless composite plating, Constitution, Structure

I. INTRODUCTION

Since the first observation by Iijima in 1991 [1], carbon nanotubes (CNTs) have been the focus of considerable research [2-6]. Numerous investigators have reported remarkable physical, mechanical and electrochemical properties of CNTs, such as unique electronic properties, high aspect ratio, outstanding thermal conductivity and strength *et al.* [7-10]. In the nature of things, CNTs are the perfect reinforce to composite materials offering tremendous opportunities for the development of mechanical and electronic industry [11-16]. Hot isostatic pressing, or powder metallurgy techniques and electroless composite plating are the conventional means to the synthesis of CNTs composite [13,17-19]. The latter is one of the important methods for CNTs composite's preparation, because it can be accomplished at low temperatures and thus avoids the interface reaction between CNTs and matrix at high temperatures. Recently, based on the sophisticated electroless Ni-P plating techniques, the research on Ni matrix-CNTs composite has been the subject of extensive investigations. Some investigations [20-25] considered that Ni-P-CNTs composite deposit had high wear resistance and low friction coefficient. However, the conformation of such kind of CNTs composites has not yet been reported and their mechanism has not been satisfactorily explained by existing theories or experiments.

In this work, the electroless composite plating has been done on the surface of copper sheet and their morphology, structure and performance have been studied.

*Author to whom correspondence should be addressed. E-mail: kongcheng@163.com

II. EXPERIMENT

A. Experimental materials and their preparation

CNTs have been synthesized by chemical vapor deposition with the diameter distributing from 30 to 50 nm and the length from 0.5 to 500 μm . In order to modify carbon nanotubes surface property and improve their dispersion in electroless composite solution, some pretreatments have been done as follows. Firstly, CNTs were greatly shortened in length by ball milling for 10 h (rotational speed 300 r/min, ratio of grinding media to material was 50 to 1); Secondly, CNTs were further oxidized for ninety minutes in the mixture of concentrated sulphuric acid and nitric acid with the volume ratio of three; Thirdly, CNTs were then sensitized for about sixty minutes in the miscible liquids of stannous chloride whose concentration is 10 g/L and some hydrochloric acid; Finally, CNTs were activated in palladium chloride with the consistency of 0.5 g/L for 1 h. Hereinbefore, each step took use of ultrasonic dispersion, followed by de-ionized water rinsing until the pH value approaches 7, vacuum filtration and drying process. The TEM images of original CNTs and processed CNTs were shown in Fig.1.

Before electroless composite plating, the copper substrate was also pretreated to ensure the quality of composite deposit, which is similar to the copper's rust removal, sanding, polishing and anneal, besides oil removal by chemical reaction, acid washing and activation.

B. The plating solution and technological parameters

An electroless plating bath was used in our experiment, consisting of nickel salt, reducing agent and some additives to maintain the process of electroless plating. Thirty-grams nickel sulphate, thirty-grams sodium hypophosphite, fifteen-grams sodium acetate and a mil-

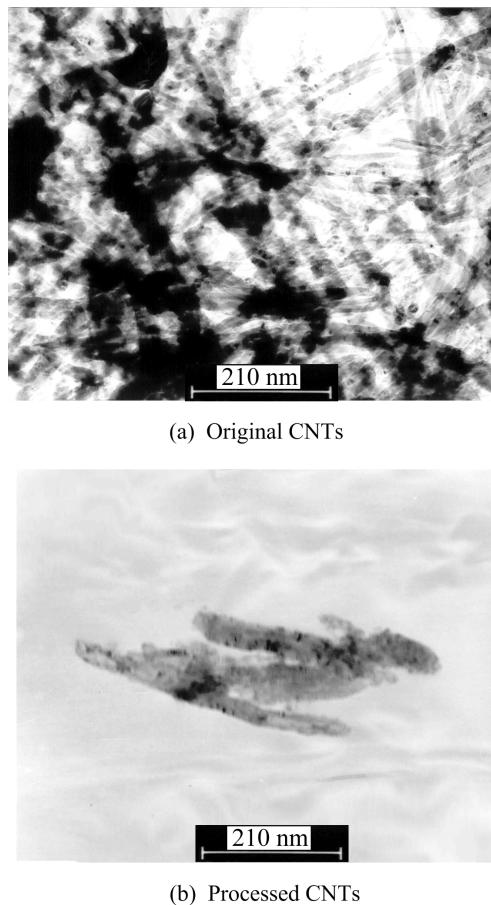


FIG. 1 TEM images of CNTs.

ligram lead acetate were added in per liter solution, as well as some proper lactic acid and citric acid acting as the complexing agent to stabilize the solution. The reaction conditions were given as follows: pH value ranging from 4.4 to 4.8, and a bath temperature at about 90 °C sustained for 5 h. There were, in addition, some cation surface-active agents, at very low concentrations, to improve the dispersion of CNTs in our plating solution.

Five groups experiments with different CNTs contents were done, and marked as 00#, 01#, 02#, 03# and 04# respectively, in which the CNTs content was 0.00, 0.25, 0.5, 0.75 and 1.00 g/L in electroless solution accordingly. The preparation procedure also included flannelette scrubbing kissingly, cleaning and dryness.

C. Microhardness

The microhardness of composite deposit was measured by HV-1000 microhardness tester. A smaller load of 0.246 N was chosen for the measurement of the composite deposit, reducing the influence of the Cu substrate to the minimum.

D. X-ray diffraction (XRD) analysis

Structural analysis of composite deposit was carried out by D/Max-1200 full automatic X-ray diffractometer. The instrument worked with the copper target and the graphite monochromator under the conditions of tube voltage 40 kV, tube current 30 mA, slit 1°-1°-0.30 mm and the scanning speed 1°/min. The diffraction angle 2θ ranged from 10° to 100°.

E. Surface morphology

Metallographic microscope and scanning electronic microscope (SEM) were adopted to observe the surface morphology of composite deposit, and EDX was used to obtain the elements distribution.

III. RESULTS AND DISCUSSION

Obviously, the processed CNTs' length is greatly shorter than the original CNTs' (Fig.1). Oxidation treatment increases the wetting ability of the CNTs surface and the number of activated sites [17]. The following surface sensibilization and activation treatment of the nanotubes with tin chloride solution and palladium chloride solution respectively results in the formation of tin or palladium particles as activated sites. From Fig.1(b), we can see that the Pd or Sn particles appear as aggregates on the outer surfaces of the nanotubes, which indicates that activated sites were formed and can initiate the deposition of nickel in the next step.

A. The surface morphology of composite deposit

The electroless Ni-P deposit is brighter than the Ni-P-CNTs composite deposit in our experiment, which can be seen by the naked eyes. The surface of electroless deposit containing CNTs was murky and gray. Figure 2 shows the metallographs for each deposit containing different CNTs content. It is not difficult to find that there are some small and nearly spheroidal islands on the surface of electroless Ni-P plating sample (Fig.2 (a)). The diameter of those evenly distributed islands varies from 2 to 10 μm. When CNTs were added, it is obvious that the diameter of the islands becomes smaller and their quantity increases (Fig.2 (b)-(e)).

Figure 3 shows the SEM images of the electroless coatings with different CNTs content. Figure 3(a) also shows the elements distribution of Ni-P electroless plating. Ni and P are the main elements on the plating surface. Carbon appears on the plating surface after CNTs were added in the electroless plating solution (Fig.3(e)). The islands (Fig.3(a)) on the electroless deposit without CNTs in the electroless plating solution are larger

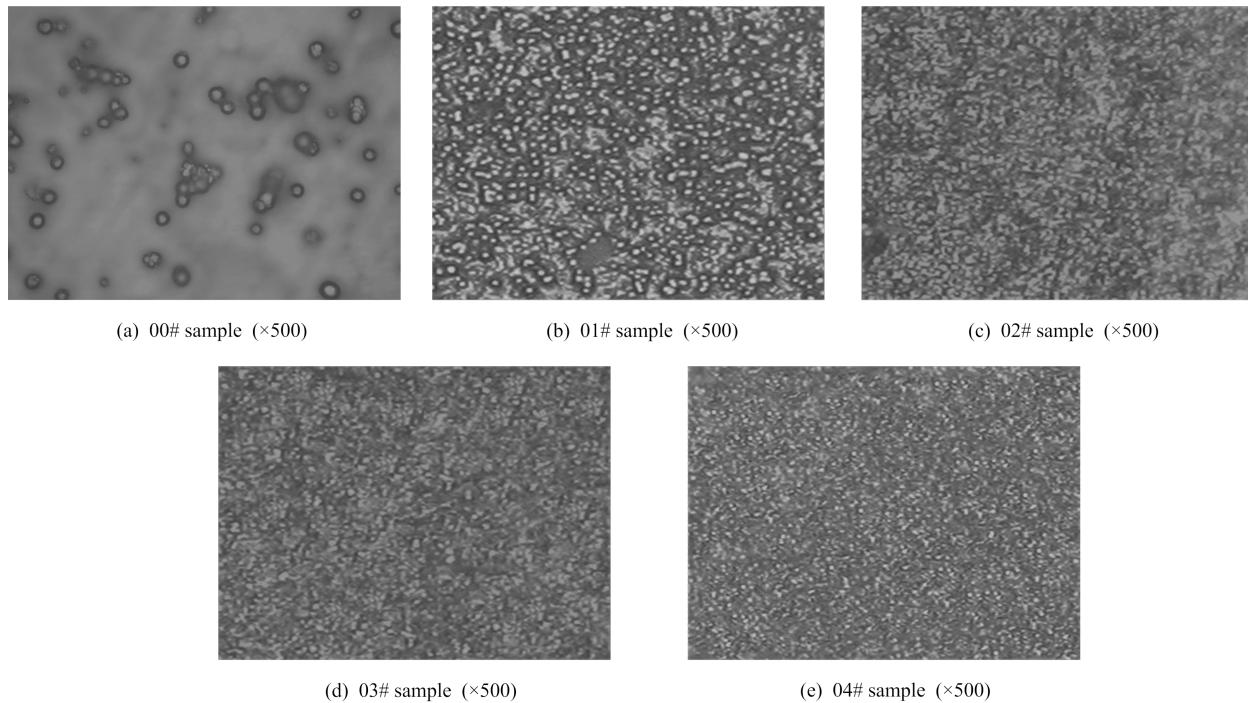


FIG. 2 Metallographs of Ni-P-CNTs samples.

than those (Fig.3 (b)-(e)) with different CNTs content. The more the CNTs content in the electroless plating solution, the smaller are the islands and the greater is the islands' density. This result is similar to that obtained from the metallographs. The increment of CNTs in electroless plating solution can clearly results in the formation of fine particles on the surface.

During the process of electroless plating, the activity of activated CNTs is higher than that of the metal matrix. Without doubt, CNTs are the nucleating and growing centers for the Ni-P alloy. The electroless plating seems to initiate on the active center of CNTs and then deposit onto the metal matrix, which results in the granular structure occurring with the center of CNTs in the electroless deposit surface. When the CNTs' concentration in electroless plating solution increases, the active center of CNTs increases. From the view of mechanism of nucleation and growth [26], it can be inferred that, under the same conditions of others, the more the initial nucleation amount, the smaller the grains. Therefore, with the increasing CNTs concentration in the electroless plating solution, the grains on the surface of electroless deposit become finer and their density is bigger.

B. Microstructure of electroless coating

Figure 4 shows the X-ray diffraction pattern for 00# samples electroless plating, and Fig.5 shows the X-ray

diffraction pattern for 01#, 02#, 03# and 04# samples electroless plating. It is noteworthy that, during the same period, the electroless Ni-P plating is thicker than the electroless Ni-P-CNTs plating. It is rather hard to obtain a very thick Ni-P-CNTs electroless plating [27]. We chose the most different part of the X-ray diffraction patterns to compare with each other. Because the Ni-P composite is thicker, only the diffraction peak of electroless deposit appears. There is a diffuse peak in the range of diffraction angle between 40° and 50° in Fig.4 and no characteristic peaks of nickel present. This indicates that electroless Ni-P plating shows amorphous state [27]. After the addition of CNTs, there are some sharp peaks in Fig.5. The stronger peaks belongs to Cu(200) and then Cu(111), and the weaker peaks to Ni(111) and then (200). These observations support that the addition of CNTs can promote the transition of electroless plating from amorphous state to crystalline state. According to broadened β of Ni(111) diffraction peak measured at half maximum of full wave (FWHM), the mosaic block size of the plating can be calculated by Scherrer-equation ($D = 0.89\lambda/\beta\cos\theta$). Table I shows the relationship between the mosaic block size of plating and the CNTs content in electroless plating solution. The grain size in electroless plating is within nanometer range and increases with the increasing CNTs content.

The electroless Ni-P plating is alloy in metastable state. At room temperature, the dissolvability of phosphorus in nickel is much limited and there's is no or less phosphorus' solid solution [27]. On the other hand,

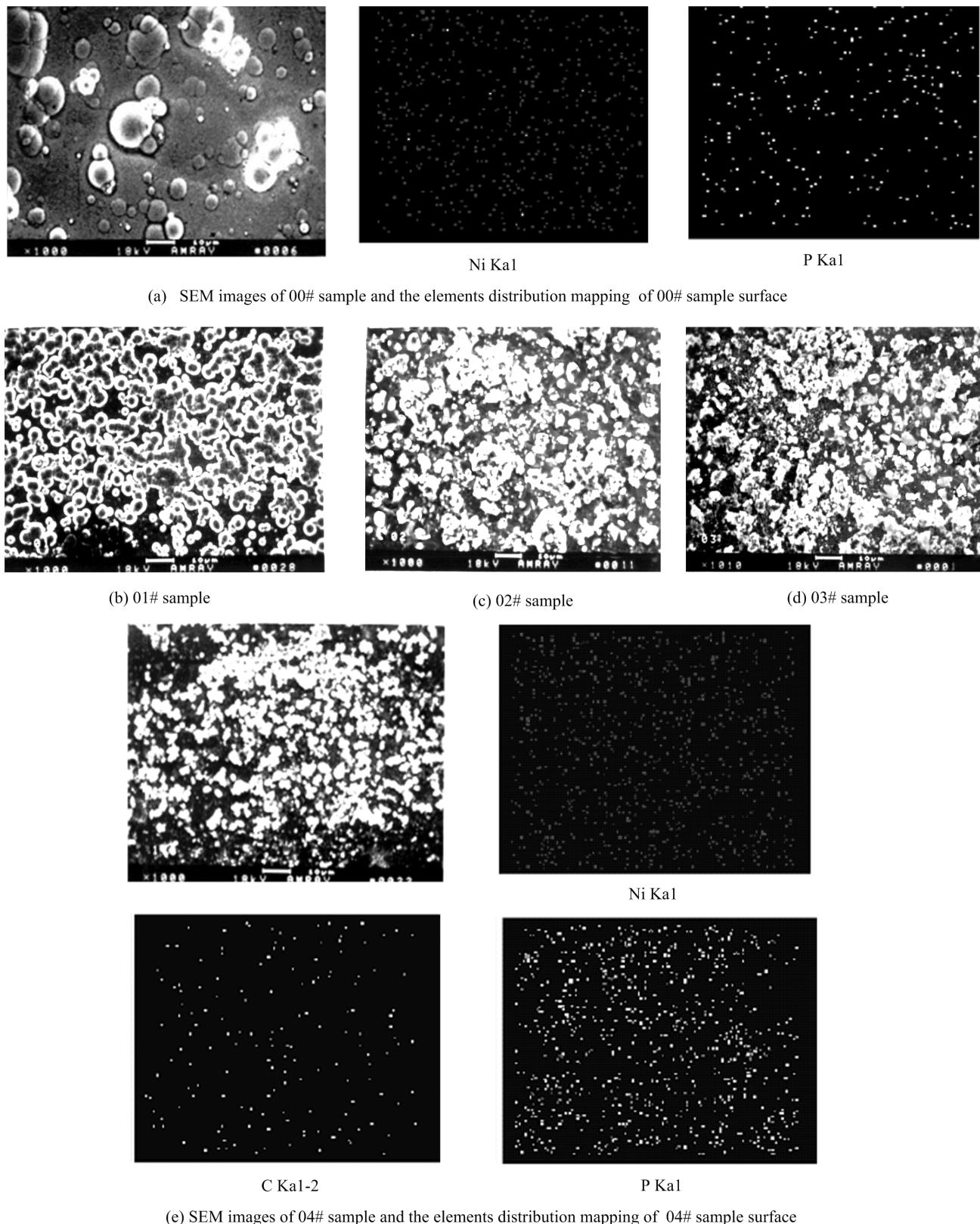


FIG. 3 SEM images of Ni-P-CNTs samples' surface.

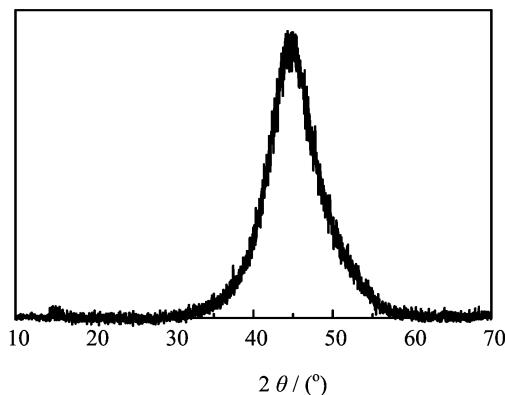


FIG. 4 Diffuse XRD pattern of Ni-P plating.

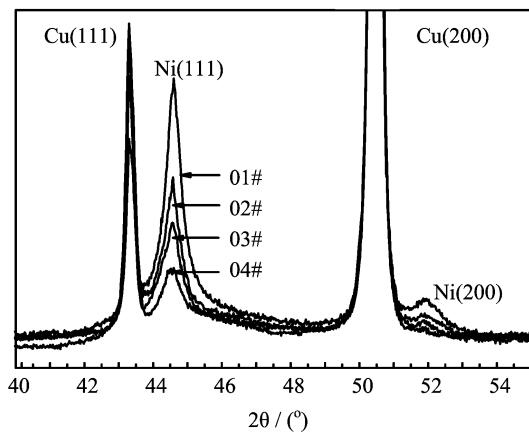


FIG. 5 XRD patterns of Ni-P-CNTs plating.

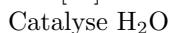
nanocrystals and amorphous solids prevent the phosphorus diffusion under the condition of our experiments. Both make the difficulty of forming Ni-P intermetallic compound. In addition, CNTs existence in the electroless plating prevents phosphorus from diffusing in nickel. Consequently, phosphorus is sandwiched between nickel and hypersaturated state in some micro-area. This results in that phosphorus content is higher in a few micro-area than their surroundings and that nickel is the mainly component in most areas. Some literatures showed that the structure of electroless Ni-P plating depends on the phosphorus content. Generally, electroless plating with the phosphorus content below seven percent shows micro-crystallite structure; with the increment of phosphorus content, the electroless plating structure changes from micro-crystallite to the amorphous state; and the electroless plating completely shows the amorphous state when the phosphorus content reaches 12 [27].

In our experiments, adding CNTs made the electroless plating structure transfer from amorphous state to nanocrystal state, demonstrating that the phospho-

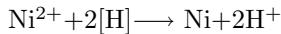
TABLE I The relationship between the mosaic block size of nanocrystal and CNTs content in electroless plating solution

Samples	01	02	03	04
CNTs content/(g/L)	0.25	0.50	0.75	1.00
Mosaic block size of nanocrystal/nm	13.4	15.2	17.3	19.1

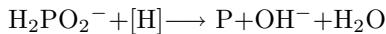
rus content decrease in nickel. Sodium Hypophosphite ($\text{NaH}_2\text{PO}_2 \cdot \text{H}_2\text{O}$) was employed as the reducing agent in the electroless plating solution. Hypophosphorous acid (H_3PO_2) is monoacid with two covalent hydrogen atoms that can not be ionized. But coexisting with catalysts such as platinum group element or iron-family elements, hypophosphorous acid radical releases active hydrogen atoms [28]. Reactions are as follows,



And some of the renascent hydrogen atom deoxidized nickel ion to metallic nickel,



The other hydrogen atom deoxidized hypophosphorous acid radical,



It is obvious that there are phosphorus atoms. Without activated CNTs, nickel and phosphorus co-deposit on the surface of samples to form Ni-P alloy plating. With activated CNTs, it is likely that phosphorus is captured by CNTs, which makes phosphorus content in nickel abate and helps the formation of nanocrystal plating.

C. Microhardness

Figure 6 shows the microhardness for the bare Cu and each sample. The average microhardness of Ni-P alloy without CNTs is greatly higher than that of Cu, but lower than the average microhardness of electroless plating with CNTs. With the increment of CNTs, the average microhardness for electroless plating increases. This strengthening could be relevant to the dispersion of CNTs in electroless plating. Moreover, the average mosaic block size of nickel is in the scale from 10 to 20 nm, i.e., nickel mainly appears as nanocrystals, contributing much to the microhardness improvement as well.

Additionally, the microhardness of the same sample is not uniform and the biggest difference is more than 100 HV. Such results can be explained by the followed reasons: on one hand, the distribution of CNTs in solution or in plating was not homogeneous. On the other hand, the distribution of phosphorus in the matrix was

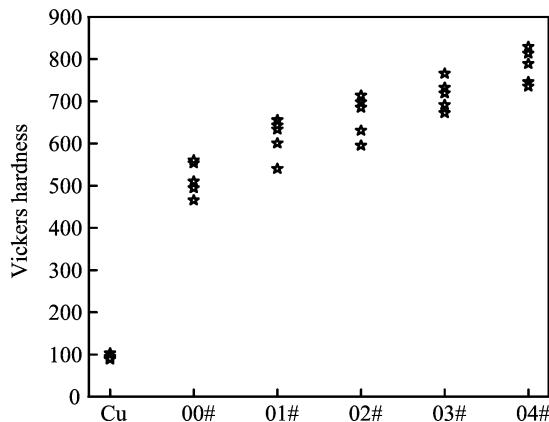


FIG. 6 Microhardness of electroless plating for each samples.

not uniform. Up to now, the two inhomogeneities cannot be avoided absolutely.

IV. CONCLUSIONS

With the increment of CNTs content in the electrodes plating solution, the grains density of the deposit surface and the plating microhardness increases, while the grain size decreases. Meanwhile, the addition of CNTs to electrodes plating solution decreases the phosphorus content in the nickel, which leads to the formation of nanocrystal in electrodes plating and promotes the crystallization of electrodes plating.

- [1] S. Iijima, Nature **354**, 56 (1991).
- [2] H. Huang, W. K. Zhang, C. A. Ma, X. B. Zhang, Z. H. Ge and H. M. Lu, Chin. J. Chem. Phys. **16**, 131 (2003).
- [3] L. Zhao, J. R. Cheng, D. C. Huang, X. H. Yuan, L. B. Zhang and R. H. Tang, Chin. J. Chem. Phys. **17**, 572 (2004).
- [4] X. F. Wang, D. B. Ruan and J. Liang, Chin. J. Chem. Phys. **18**, 421 (2005).
- [5] J. F. Chen, C. L. Xu, Z. Q. Mao, G. R. Chen, B. Q. Wei, J. Liang and D. H. Wu, Sci. Chin. Ser. A **45**, 82 (2002).
- [6] Y. H. Li, J. Ding, J. F. Chen, C. L. Xu, B. Q. Wei, J. Liang and D. H. Wu, Mater. Res. Bull. **37**, 313 (2002).

- [7] S. Iijima, C. Brabec, A. Maiti and J. Bernholc, J. Chem. Phys. **104**, 2089 (1996).
- [8] M. B. Nardelli, J. L. Fattebert, D. I. Orlikowsk, et al. Carbon. **38**, 1703 (2000).
- [9] Z. L. Wang, R. P. Gao, P. Poncharal, et al. Mater. Sci. Eng. C **16**, 3 (2001).
- [10] R. H. Baughman, A. A. Zakhidov and W. A. Deheer, Science **297**, 781 (2002).
- [11] J. H. Fan, M. X. Wan, D. B. Zhu, B. H. Chang, Z. W. Pan and S. S. Xie, Synthetic Metals **102**, 1266 (1999).
- [12] J. M. Park, D. S. Kim, J. R. Lee and T. W. Kim, Mater. Sci. Eng. C **23**, 971 (2003).
- [13] W. X. Chen, J. P. Tu, L. Y. Wang, H. Y. Gan, Z. D. Xu and X. B. Zhang, Carbon **41**, 215 (2003).
- [14] Y. Breton, G. D esarmot, J. P. Salvatet, S. Delpeux, C. Sinturel, F. B eguin and S. Bonnamy, Carbon **42**, 1027 (2004).
- [15] L. P. Zhao and L. Gao, Carbon **42**, 423 (2004).
- [16] M. K. Yeh, N. H. Tai and J. H. Liu, Carbon **44**, 1 (2006).
- [17] X. H. Chen, J. T. Xia, J. C. Peng, W. Z. Li and S. S. Xie, Compos. Sci. Technol. **60**, 301 (2000).
- [18] S. R. Dong, J. P. Tu and X. B. Zhang, J. Zhejiang Univ. (Eng. Sci.) **35**, 29 (2001).
- [19] Cs. Balázsi, Z. Kónya, F. Wéber, L. P. Biró and P. Arató, Mater. Sci. Eng. C **23**, 1133 (2003).
- [20] W. X. Chen, H. Y. Gan, J. P. Tu, W. L. Chen, J. S. Xia, J. G. Wang, Z. D. Xu and G. Z. Zhou, Tribology **22**, 241 (2002).
- [21] W. S. Lin, X. Y. Zhou, S. J. Wang and Y. Li, J. Mater. Sci. Eng. **23**, 218 (2005).
- [22] H. Xu, J. Zhai, M. K. Li and H. L. Li, J. Lanzhou Univ. Technolo. **30**, 70 (2004).
- [23] L. Y. Wang, J. P. Tu , W. X. Chen, Y. C. Wang, X. K. Liu, Charls Olk, D. H. Cheng and X. B. Zhang, Wear **254**, 1289 (2003).
- [24] W. X. Chen, J. P. Tu, H. Y. Gan, Z. D. Xu, Q. G. Wang, J. Y. Lee, Z. L. Liu and X. B. Zhang, Surf. Coat. Technolo. **160**, 68 (2002).
- [25] X. H. Chen, C. S. Chen, H. N. Xiao, F. Q. Cheng, G. Zhang and G. J. Yi, Surf. Coat. Technolo. **191**, 351 (2005).
- [26] R. R. Song and W. M. Sui, J. Cerami. **25**, 186 (2004).
- [27] N Li, *Practical Technology on Electroless Plating*, Beijing: The Chemical Industry Press, 176 (2004).
- [28] Q. L. Xu, *Contemporary Surface Treatment New Technology*, Shanghai: Science and Technology Press of Shanghai, 511 (1994).